

Quantification of fluorophore concentration *in vivo* using two simple fluorescence-based measurement techniques

Kevin R. Diamond
Pawel P. Malysz
Joseph E. Hayward
Michael S. Patterson

Juravinski Cancer Centre and McMaster University
Department of Medical Physics
699 Concession Street
Hamilton, Ontario, Canada L8V 5C2
E-mail: kevin.diamond@hrcc.on.ca

Abstract. The effect of photodynamic therapy treatments depends on the concentration of photosensitizer at the treatment site; thus a simple method to quantify concentration is desirable. This study compares the concentration of a fluorophore and sensitizer, aluminum phthalocyanine tetrasulfonate (AlPcS₄), measured by two simple fluorescence-based techniques *in vivo* to *post mortem* chemical extraction and fluorometric assay of those tissues: skin, muscle, fascia, liver, and kidney (cortex and medulla). Fluorescence was excited and detected by a single optical fiber, or by an instrument that measured the ratio of the fluorescence and excitation reflectance. The *in vivo* measurements were compared to calibration measurements made in tissue-simulating phantoms to estimate the tissue concentrations. Reasonable agreement was observed between the concentration estimates of the two instruments in the lighter colored tissues (skin, muscle, and fascia). The *in vivo* measurements also agreed with the chemical extractions at low (<0.6 $\mu\text{g/g}$) tissue concentrations, but underestimated higher tissue concentrations. Measurements of fluorescence lifetime *in vivo* demonstrated that AlPcS₄ retains its mono-exponential decay in skin, muscle, and fascia tissues with a lifetime similar to that measured in aqueous tissue-simulating phantoms. In liver and kidney an additional short lifetime component was evident. © 2005 Society of Photo-Optical Instrumentation Engineers. [DOI: 10.1117/1.1887932]

Keywords: fluorescence; fluorophore concentration; fluorescence lifetime; *in vivo*; photodynamic therapy; tissue optics.

Paper 04131 received Jul. 12, 2004; revised manuscript received Oct. 20, 2004; accepted for publication Nov. 2, 2004; published online May 4, 2005.

1 Introduction

The use of fluorescence as a quantitative tool for measuring fluorophore concentrations in turbid media such as tissue is growing. Various clinical applications have been explored including pharmacokinetics¹⁻³ and photosensitizer dosimetry for photodynamic therapy (PDT).⁴⁻⁶ Since the yield of the photochemical reactions important to photodynamic therapy is dependent on the photosensitizer concentration, an accurate method to rapidly determine this quantity is desirable.

The fluorophore concentration in tissues is usually determined by invasive procedures such as drawing blood or taking biopsies and performing analysis (such as chemical extraction) on the sample. A variety of less invasive approaches to fluorophore quantification (and hence photosensitizer dosimetry) have been attempted based on absorption and fluorescence spectroscopy. Weersink et al.⁷ measured photosensitizer concentration by *in vivo* reflectance spectroscopy on rabbits injected with aluminum phthalocyanine tetrasulfonate (AlPcS₄). Measurements on the liver yielded accurate con-

centration estimates, but concentration estimates in skin were affected by its multilayered structure. Mourant et al.⁸ measured tissue concentrations of chemotherapy drugs (Doxorubicin and Mitoxantrone) in an animal tumor model system, using a single optical fiber source-detector pair to measure absorption. The separation of the source and detector fibers—was chosen to minimize the dependence of the detected optical signal on the tissue scattering properties. The measured concentrations were linear with the extracted concentrations but systematically underestimated the true value as determined by chemical extraction, possibly due to inadequacies of the theoretical model they employed.

Other quantification techniques rely on the measurement of fluorescence. Panjehpour et al.⁴ showed that sulphonated aluminum phthalocyanine fluorescence measured in rats depended linearly on concentration, which was determined by chemical extraction of tissue samples. A more recent study by Lee et al.⁹ compared measurements of AlPcS₂ concentration using a fiber bundle probe¹⁰ to a chemical extraction technique. They used measurements of concentration *in vivo* to calibrate the probe, and used that calibration to quantify up-

Address all correspondence to Kevin Diamond, Medical Physics, Juravinski Cancer Centre and McMaster University, 699 Concession Street, Hamilton, ON L8V 5C2 Canada; Tel: 905-387-9711 x67145; Fax: 905-575-6337; E-mail: kevin.diamond@hrcc.on.ca

take in muscle and liver. Some discrepancies were noted and were attributed to changes in the fluorescence quantum yield, changes in the partitioning of the fluorophore between blood and tissue, and absorption of the excitation light by hemoglobin.

The goal of this paper is to examine the accuracy of concentration estimates of the fluorophore and photosensitizer, aluminum phthalocyanine tetrasulfonate (AIPcS₄), injected intravenously into New Zealand White (NZW) rabbits. Two fluorescence-based methods of quantitation, both of which minimized the dependence of the concentration estimates on the optical properties, were compared to a chemical extraction protocol.¹¹ The first method was described by Weersink et al.¹² and uses the ratio of the fluorescence and the scattered excitation light detected at two source detector separations, ρ_f and ρ_x respectively. The optimal distances ($\rho_f=0.65$ mm and $\rho_x=1.35$ mm) were chosen to minimize the root-mean-square percent error in the concentration estimate over a wide range of optical properties. Prior to the construction of a probe, preliminary measurements of *in vivo* fluorescence were made on a single rabbit using the ratio technique with selections of $\rho_f=0.86$ mm and $\rho_x=1.42$ mm (from an existing probe) and showed that the ratio technique could estimate fluorophore concentration accurately in skin, liver and muscle tissue. A new probe was designed based on the optimal source-detector separations and was used in this study.

The second method used a single optical fiber to excite and detect fluorescence and has been described previously.¹³ A single optical fiber has the advantage of being implantable for interstitial measurements. For the single fiber measurements reported here, time-resolved fluorescence was measured rather than steady-state fluorescence as in the original study.¹³ By measuring the time-resolved fluorescence, the fluorescence lifetime can be obtained *in vivo*. The fluorescence lifetime is an important component of this study because it is related to the fluorescence quantum yield, which may be different in tissues than in external calibration standards.^{9,13} Differences in the fluorescence quantum yield could be erroneously interpreted as differences in fluorophore concentration. Changes in the fluorescence lifetime, however, do not necessarily reflect physical changes (e.g., interactions that cause the fluorophore to become nonfluorescent) that the fluorophore may undergo *in vivo* and which could also affect the fluorescence quantum yield.

A recent study by Vishwanath et al.¹⁴ showed that the fluorescence lifetime measured using a probe comprised of a bundle of small diameter optical fibers¹⁰ did not depend on the optical properties of the tissue-simulating phantoms used. This result suggests that any differences between the fluorescence lifetime measured in tissue and in the calibration standards should be due to the differences in the local fluorophore environment and hence related to changes in the quantum yield. Some changes in the fluorescence quantum yield (due to collisional quenching for example) may be corrected by using the ratio of the fluorescence lifetime measured *in vivo* to the lifetime measured in the calibration phantom. The study,¹⁴ however, did not address the situation of a fiber implanted in a turbid medium, which we examine in this paper.

2 Materials and Methods

2.1 Fluorophore Preparation

Aluminum phthalocyanine tetrasulfonate (AIPcS₄) was purchased from Porphyrin Products (Logan, Utah). The compound was dissolved in 0.9% sterile saline and was used as a stock solution for administration to the animals and measurements in tissue-simulating phantoms.

2.2 Animal Procedures

Sixteen New Zealand White (NZW) specific-pathogen free (SPF) rabbits weighing 2 to 4 kg were used. Rabbits were weighed and then injected with the desired dose of AIPcS₄, which ranged from 0.5 to 4 mg/kg. One rabbit was injected with 1 mL of sterile 0.9% saline as a control. Fluorescence measurements were performed under general anesthetic 18 to 28 hours after the injection of the fluorophore. The animals were initially anesthetized with an intramuscular injection of lidocaine hydrochloride (Xylazine®, 4 mg/kg), followed by an injection 10 min later of a mixture of ketamine hydrochloride (Ketalean®, 40 mg/kg) and acepromazine maleate (Atravet®, 0.75 mg/kg). Anesthesia was maintained by gaseous anesthetic (isoflurane, 1.5%) for 12 rabbits, and by injections of the Ketalean®/Atravet® mixture for the other four. Animal ethics approval was obtained for these experiments.

2.3 Experimental Apparatus

Estimates of fluorophore concentrations were performed using two different instruments. The first instrument used the fluorescence/reflectance (F/R) ratio to estimate fluorophore concentrations. A schematic for this instrument is shown in Fig. 1. The excitation light source was a 640-nm steady-state diode laser (OZ Optics, Ottawa, Ontario). The laser was coupled to the source fiber of a fiber-optic probe (Fiberguide Industries, Stirling, New Jersey) which had two detection fibers with source-detector separations of 0.65 mm and 1.35 mm. The detection fibers were connected to an Ocean Optics (Dunedin, Florida) SD2000 dual channel CCD spectrometer. A 665-nm cut-on filter (Oriel, Stratford, Connecticut) was used in the fluorescence channel to reduce the intensity of the excitation line. A background spectrum obtained from the skin surface with the laser turned off was subtracted from all measured spectra. The instrument was interfaced to a laptop computer where the data were processed and displayed. The excitation component of the reflectance signal was measured by integrating the spectrum from 635 to 645 nm. The fluorescence signal was the integral from 675 to 685 nm. A sample spectrum is shown as an inset to Fig. 1, with the fluorescence integration limits indicated.

The second instrument was based on exciting and detecting time-resolved fluorescence using a single optical fiber. A schematic of the apparatus is shown in Fig. 2. A 635-nm pulsed diode laser (BHL-150, Becker & Hickl, Germany) was used to excite the fluorophore. The laser had a repetition rate of 50 MHz and a pulse width of approximately 150 ps. Light from the laser was coupled into a mirror assembly (ThorLabs, Newton, New Jersey) that separated fluorescence from the excitation light using a thin dichroic mirror (Oriel, Stratford, Connecticut). The mirror/lens assembly coupled the excitation light into a single 200- μ m optical fiber probe, which was used to excite and detect the fluorescence. The fluorescence col-

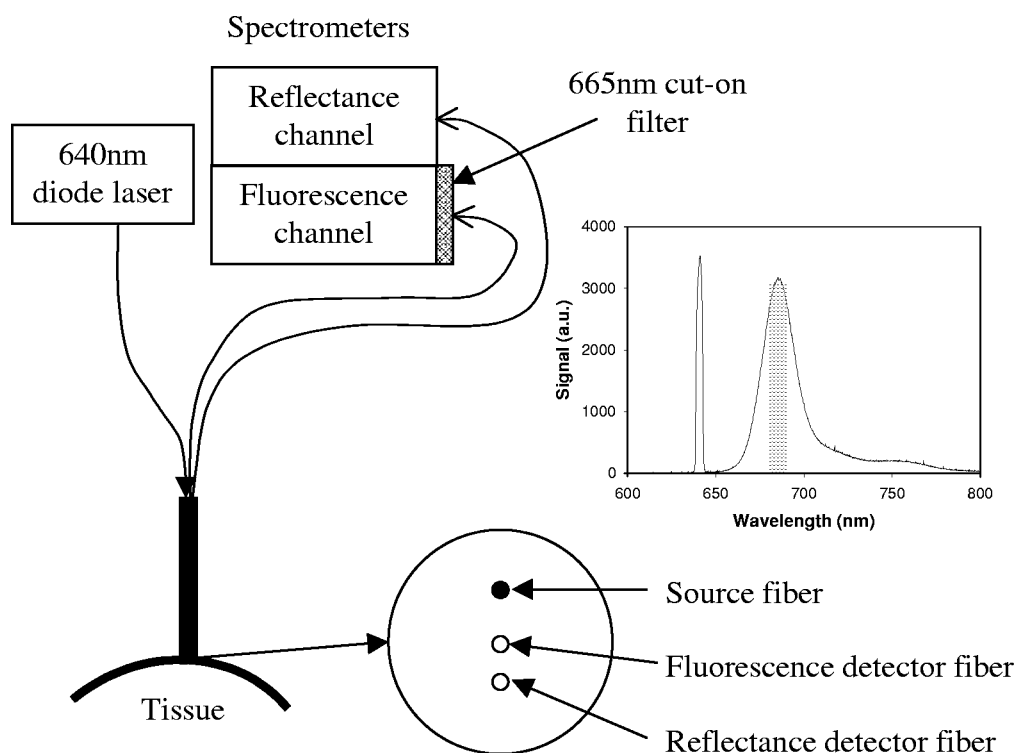


Fig. 1 Experimental apparatus for F/R ratio measurements. The optical fibers of the F/R probe were 200 μm in diameter. The inset spectrum is an overlay of the fluorescence and reflectance channels. The region of integration for the fluorescence channel is shaded gray.

lected by the probe was reflected from the mirror into an optical fiber coupled to a photomultiplier tube (H5783P-01, Hamamatsu, Bridgewater, New Jersey). The fluorescence was filtered with 665-nm cut-on and 680-nm band-pass filters (Oriol, Stratford, Connecticut) to reduce the signal from scattered excitation light (from the mirror and the sample) and to limit the spectral width of the detected fluorescence. The pulse from the photomultiplier tube was amplified, time delayed, and used as a “start” input to a time-correlated single photon counting card (SPC-630, Becker & Hickl, Germany)

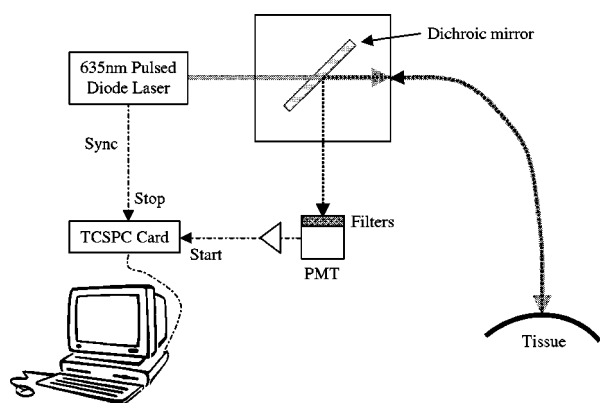


Fig. 2 Experimental apparatus for single fiber measurements. The solid gray line is the excitation path and the dotted line the fluorescence. Dash-dots are electrical connections. The time-correlated single photon counting (TCSPC) module was run in reverse time mode, with the time measurement started by the detection of a photon, and stopped by the synchronization pulse from the laser.

operated in reversed “start-stop” mode. The “stop” input was from an electronic synchronization pulse from the laser driver.

2.4 Measurements in Tissue-Simulating Phantoms

Measurements using the F/R and single fiber instruments *in vivo* were compared to separate calibration measurements. These were made on tissue-simulating phantoms with five combinations of optical properties containing known concentrations of AlPcS₄. The optical properties of the phantoms at 635 nm were $\mu'_s=0.6 \text{ mm}^{-1}$, $\mu_a=0.001 \text{ mm}^{-1}$; $\mu'_s=0.6 \text{ mm}^{-1}$, $\mu_a=0.1 \text{ mm}^{-1}$; $\mu'_s=1.2 \text{ mm}^{-1}$, $\mu_a=0.01 \text{ mm}^{-1}$; $\mu'_s=2.4 \text{ mm}^{-1}$, $\mu_a=0.001 \text{ mm}^{-1}$; $\mu'_s=2.4 \text{ mm}^{-1}$, $\mu_a=0.1 \text{ mm}^{-1}$. The tissue-simulating phantoms comprised a dilute aqueous suspension of Higgins India ink (Eberhard Faber Inc., Lewisburg, Tennessee) for absorption and Intralipid-20% (Pharmacia Corporation, Peapack, New Jersey) for scattering. The concentrations of ink and Intralipid-20% required to achieve these combinations of optical properties were determined in previously published work.¹⁵ AlPcS₄ concentrations ranging from 0.1 to 5.0 $\mu\text{g}/\text{mL}$ were added to the phantoms prior to fluorescence measurements.

The line of best fit to the measured signal (either F/R or the time-integrated fluorescence measured with the single optical fiber) versus concentration for all phantoms was used to estimate tissue concentrations from *in vivo* measurements. Note that both techniques minimize the dependence of signal on optical properties so that a single calibration curve can be used for the wide range of μ'_s and μ_a . The measured time-resolved fluorescence curves contained contributions due to the fluorophore and instrumental autofluorescence (which was measured when tissue-simulating phantoms containing no

AlPcS₄ were used). The fluorescence due to AlPcS₄ was the difference of these two curves (each curve normalized to the collection time). The area under this difference curve was the total fluorescence signal used for determining concentration. The fluorescence lifetime was estimated using a weighted least-squares fit to a single exponential decay.¹⁶

2.5 Measurements In Vivo

Fluorescence measurements were performed at several locations on the rabbits. The two instruments were used sequentially to prevent optical cross talk. Sites on the skin were located on the back (over the dorsal muscle) and on the leg. These sites were shaved and then depilated with a hair removal product (Nair®). After data were acquired for the skin, an incision was made and the skin reflected to expose the underlying muscle. Fluorescence was measured on the muscle in roughly the same locations as on the overlying skin. Interstitial measurements in muscle (fiber embedded ~5 mm below the surface) were also performed using the single optical fiber. An 18-gauge needle was used to guide the fiber into the muscle, and was removed before commencing the fluorescence measurement. After sacrifice, the liver and kidney were surgically exposed. Measurements were performed on the surface (F/R and single fiber) and interstitially (the end of the fiber placed 2 to 3 mm into the organ using the same technique as in muscle). Skin and muscle samples were harvested from the marked measurement sites immediately after sacrifice, and from the liver and kidney shortly after the measurements were performed. The tissue samples were stored at -80 °C for subsequent chemical extraction.

The background for the time-resolved system was the average of the signal measured with the fiber tip in water and in air. This was found to be close to the signal found for the control (no AlPcS₄ injected) animal. Time-resolved data were fitted to either a single or double exponential decay.¹⁶ For those data fitted with a double exponential decay, the time integrated fluorescence signal, F , was corrected for shorter lifetimes. The corrected fluorescence signal is given by the expression:

$$F_{corr} = F \left(f_{long} \frac{\tau_o}{\tau_{long}} + f_{short} \frac{\tau_o}{\tau_{short}} \right) \quad (1)$$

where f_{long} and f_{short} are the fractional contributions of the long and short lifetime components (τ_{long} and τ_{short}) to the time integrated fluorescence signal, and τ_o is the lifetime in the calibration phantom (5.25 ns).

2.6 Chemical Extractions

Measurements of concentration in tissue were performed by fluorimetry based on the extraction protocol of Lilge et al.¹¹ Three samples were cut from each piece of harvested tissue, each weighing approximately 0.1 g, and 1 mL of Solvable™ tissue solubilizer (Packard Bioscience BV, Groningen, the Netherlands) was added to each piece. Mechanical homogenization was performed by sonification (Sonics & Materials Inc., Danbury, Connecticut) at intervals of 60 to 90 sec, until no large tissue fragments remained. An additional aliquot of 1 mL of Solvable™ was added to the sonicator tip to avoid tissue mass loss. The samples were then placed in a 50 °C

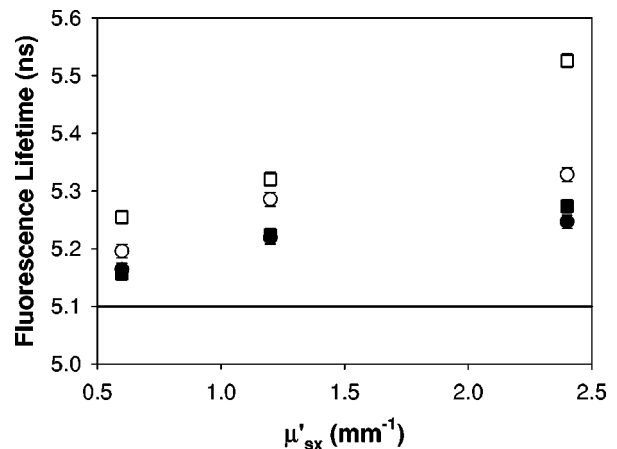


Fig. 3 AlPcS₄ fluorescence lifetime measured in aqueous tissue-simulating phantoms. Squares represent interstitial measurements, circles measurements at the surface. Open and closed symbols represent $\mu_a = 0.001 \text{ mm}^{-1}$ and $\mu_a = 0.1 \text{ mm}^{-1}$ respectively. The solid line is the fluorescence lifetime measured in cuvettes of 0.9% saline.

shaking water bath for 2 to 3 hours. All samples were transparent by this time. Five known concentrations of AlPcS₄ were taken from the stock solution (after dilution in 0.9% saline) and processed in the manner described above. The fluorescence signals from these known concentrations were used to calibrate the spectrometer. Four 100- μL aliquots of each of these samples were diluted into 2 mL of double-distilled water, and the fluorescence from these dilutions was measured. This dilution ensured that the optical density of all samples at the excitation wavelength was less than 0.1 so that correction for optical absorption within the sample was unnecessary.¹¹

3 Results

3.1 Calibration Measurements in Tissue-Simulating Phantoms

Measurements were performed on tissue-simulating phantoms to calibrate the F/R ratio and time-resolved single fiber instruments. The calibration line for the F/R probe was the best fit straight line for the five combinations of optical properties (in Section 2.4) over the range of fluorophore concentrations. The root-mean-square percent error in the calibration line was 16.5%. The calibration of the single fiber probe, using both surface and interstitial measurements, yielded root-mean-square errors of 11%. These measurements are not shown here because they were very similar to the data presented in the papers^{12,13} that describe each technique in detail. An additional calibration, with baseline absorption coefficients ranging from approximately 0.2 to 0.5 mm^{-1} ($\mu'_{sx} = 1.2 \text{ mm}^{-1}$), was performed for use with the liver and kidney measurements, because the absorption coefficient for these two organs was anticipated to be well outside the range of μ_a used to develop calibration curves in previous studies.^{12,13}

Estimates of the fluorescence lifetime were made for each combination of optical properties and fluorophore concentration. These data are shown in Fig. 3, plotted as a function of the reduced scattering coefficient at the excitation wavelength. The horizontal line on the graph represents the mean fluores-

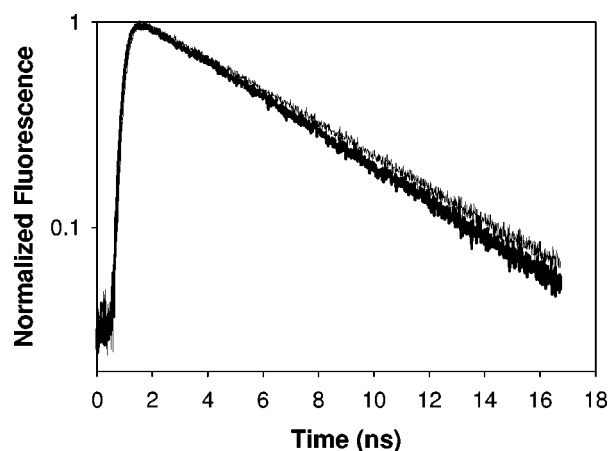


Fig. 4 Time-resolved fluorescence curves measured in aqueous tissue-simulating phantoms. The thin line represents an interstitial measurement for $\mu'_{sx}=2.4 \text{ mm}^{-1}$ and $\mu_a=0.001 \text{ mm}^{-1}$. The thick line represents a surface measurement for $\mu'_{sx}=0.6 \text{ mm}^{-1}$ and $\mu_a=0.1 \text{ mm}^{-1}$. Both phantoms contain $2 \mu\text{g}/\text{mL}$ AlPcS₄.

cence lifetime (\pm standard error in the mean), 5.10 ± 0.02 ns, measured in clear solutions at four concentrations using the same stock of AlPcS₄. The fluorescence lifetime measured at the surface of the phantoms was slightly dependent on the optical properties, with values (\pm standard error in the mean, six concentrations, and three measurements per concentration) ranging from 5.16 ± 0.01 ns ($\mu'_{sx}=0.6 \text{ mm}^{-1}$, $\mu_a=0.1 \text{ mm}^{-1}$) to 5.33 ± 0.01 ns ($\mu'_{sx}=2.4 \text{ mm}^{-1}$, $\mu_a=0.001 \text{ mm}^{-1}$). Interstitial measurements yielded results that were more dependent on the optical properties. In this configuration, the measured fluorescence lifetime ranged from 5.16 ± 0.01 ns ($\mu'_{sx}=0.6 \text{ mm}^{-1}$, $\mu_a=0.1 \text{ mm}^{-1}$) to 5.53 ± 0.01 ns ($\mu'_{sx}=2.4 \text{ mm}^{-1}$, $\mu_a=0.001 \text{ mm}^{-1}$). The difference in the measured (apparent) fluorescence lifetime between the interstitial and surface geometries for the $\mu'_{sx}=2.4 \text{ mm}^{-1}$, $\mu_a=0.001 \text{ mm}^{-1}$ phantom was possibly a result of long path-length photons scattered from behind the plane of the flatcut end of the fiber. The surface and interstitial time-resolved curves for the $\mu'_{sx}=0.6 \text{ mm}^{-1}$, $\mu_a=0.1 \text{ mm}^{-1}$ (surface) and $\mu'_{sx}=2.4 \text{ mm}^{-1}$, $\mu_a=0.001 \text{ mm}^{-1}$ (interstitial) phantoms are shown in Fig. 4. The instrumental autofluorescence has been subtracted from each of the curves, and the data normalized to the maximum value for comparison. Even in this extreme comparison the influence of the geometry (interstitial versus surface) and optical properties on the lifetime was only 0.3 ns.

3.2 Specific Uptake of AlPcS₄ in Various Tissues

The specific uptake was determined for each tissue type by dividing the results of the chemical extraction by the injected dose. (The injected doses for the first four rabbits were unavailable). The specific uptake in the various tissues measured in this study were consistent with other reported values for NZW rabbits^{7,12} and are shown in Fig. 5. The specific uptake of AlPcS₄ in skin, muscle, and liver reported in Ref. 12 were from a single rabbit and so should be interpreted with caution given the inter-animal variation evident in Fig. 5. The specific uptake in skin was 0.53 ± 0.05 as determined by the slope of the best-fit line [Fig. 5(a)]. This is comparable to the value of

0.41 ± 0.02 measured in Ref. 7. The specific uptake from the rabbit measured in Ref. 12 was approximately 0.7 ± 0.1 , as determined by measuring at five different skin sites. Studies in rodents have produced a range of specific uptake for AlPcS₄ ranging from 0.09 in mouse skin¹⁷ to 1.02 in rat skin,¹⁸ both determined at 24 hours post-administration. The uptake of AlPcS₄ for muscle (both leg and dorsal muscle) and fascia are shown in Figs. 5(b) and 5(c), respectively. Values of AlPcS₄ uptake in fascia were not available from the literature, but the measured specific uptake for these measurements was 0.39 ± 0.05 . The specific uptake in muscle was 0.062 ± 0.006 , which is consistent with a reported value of 0.052 ± 0.008 .⁷ However, the specific uptake reported in Ref. 12 was approximately 0.15 ± 0.05 . Measurements in rodents by other researchers produced a range of specific uptake for muscle: two studies determined that the specific uptake in rat muscle was 0.14 (Ref. 19) and 0.46 (Ref. 18), while the specific uptake in mouse muscle was 0.02.¹⁷ Liver [Fig. 5(d)] retained considerably more of the fluorophore, with a specific uptake of 2.2 ± 0.1 . This compared well to the single rabbit of Ref. 12, where the specific uptake in liver was approximately 2.00 ± 0.05 , but was about twice the value measured in Ref. 7, 0.89 ± 0.08 . Our measured value fell between those reported for other rodents, which ranged from approximately 1.2 in rats¹⁹ to 3.5 in mice.¹⁷ In kidney [Fig. 5(e)], we measured a specific uptake of 3.0 ± 0.2 . This value is considerably higher than the measured values in two mouse models, where a specific uptake of approximately 0.2 was measured in BALB/c mice,¹⁷ and a specific uptake of 0.7 was measured in a later study by the same group in the same model system.²⁰ It should be noted that a much lower specific uptake, 0.78 ± 0.07 , was measured at the core of the kidney [Fig. 5(f)].

3.3 Quantitative Measurements In Vivo

The fluorescence lifetimes determined by the time-resolved instrument are shown in Fig. 6. The standard error in the mean for the individual data points (determined from at least three repeated measurements) ranged from 0.05 to 0.2 ns (error bars not shown). In skin, muscle, and fascia, the fluorescence decay was fitted using a single exponential decay. In liver and kidney, a double exponential decay was required to fit the data. The mean values (\pm standard error in the mean) of the fluorescence lifetimes shown in Fig. 6 are presented below.

The tissue concentrations measured by the single fiber probe and the F/R ratio probe were compared with concentrations determined by chemical extraction. The concentration estimates for the skin, muscle and fascia are shown in Fig. 7. Horizontal error bars were derived from extractions from three samples cut from the tissue harvested from the measurement site. Measurements made on skin on the back and on the leg are shown in Fig. 7(a). Measurements with the single optical fiber and the F/R probe yielded similar results except at the highest concentrations. The average fluorescence lifetime measured in skin was 5.00 ± 0.06 ns. Measurements with the two probes were in good agreement with the chemical extractions at low concentrations ($<0.6 \mu\text{g}/\text{g}$) but underestimated the tissue concentration at higher injected doses of AlPcS₄. Measurements in muscle are shown in Fig. 7(b). The average lifetime measured in muscle (including both the surface and interstitial geometries) was 5.09 ± 0.08 ns. The measured con-

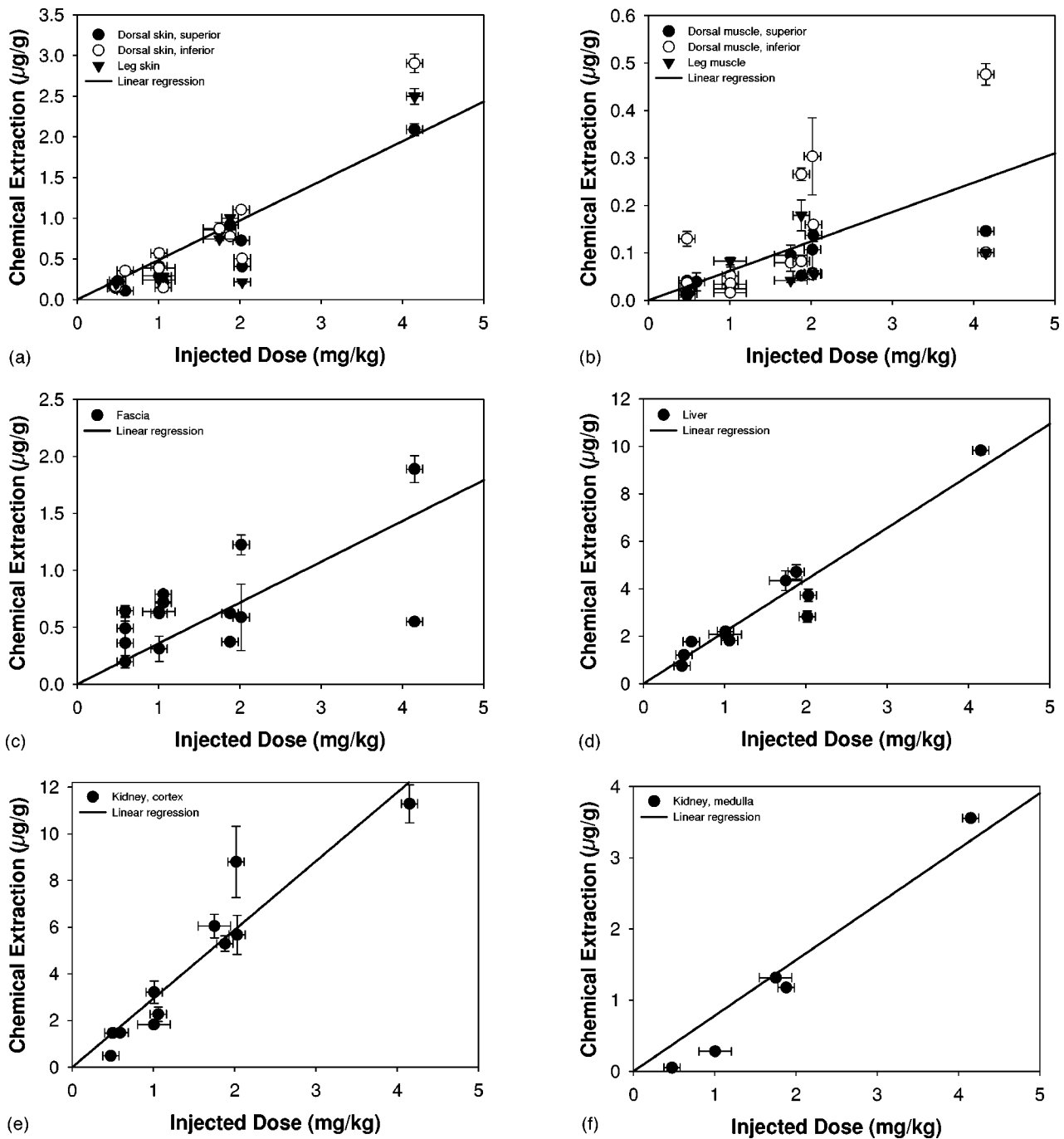


Fig. 5 The specific uptake of AlPcS₄ measured in (a) skin, (b) muscle, (c) fascia, (d) liver, (e) kidney cortex, and (f) kidney medulla. The tissue sites corresponding to the different symbols are shown in each panel. Horizontal error bars were based on the uncertainty in the mass of the rabbits and the quantity of the fluorophore injected. The vertical error bars are the standard error in the mean for 12 total measurements of the three tissue samples taken from the measurement site.

centration was scattered around the line of equality, with the majority of the measurements showing very low concentrations ($<0.1 \mu\text{g/g}$). Figure 7(c) shows the measured concentration of AlPcS₄ in fascia. Both single fiber and F/R probes tended to underestimate the concentration, but were in good agreement with one another. The average fluorescence lifetime measured from the fascia sites was $5.1 \pm 0.1 \text{ ns}$.

Measurements made on liver immediately *post mortem* using a separate high-absorption calibration are shown in Fig. 8.

Figure 8(a) shows the measured concentrations compared to the chemical extractions. Both the F/R ratio probe and the single fiber tended to underestimate the concentration, but the single fiber measurements were more accurate. The average long and short lifetime components measured in the liver were $5.0 \pm 0.1 \text{ ns}$ and $1.62 \pm 0.06 \text{ ns}$ respectively. The short lifetime component of the fluorescence contributed approximately 10% of the integrated signal. Figure 8(b) shows a comparison of the concentration measured using the single

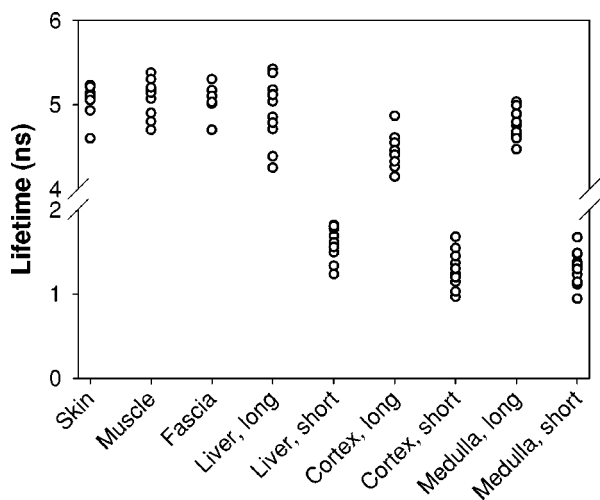


Fig. 6 The scatter plot shows the average fluorescence lifetime (three measurements) from the various tissues in 11 rabbits. The standard error in the means ranged from 0.05 to 0.2 ns, error bars not shown.

fiber with and without a correction performed to account for the quenching associated with the short lifetime component. The ratio of the slopes between the two linear regressions (corrected for lifetime compared to not corrected) is approximately 1.27. Similar results (also using the separate calibration) were observed in kidney. Figure 9(a) shows the concentration of ALPcS₄ measured by the single fiber and F/R ratio probes. Both probes underestimated the concentration. The average fluorescence lifetimes measured in the cortex were 4.40 ± 0.04 ns and 1.28 ± 0.07 ns. Interstitial kidney (medulla) measurements had slightly different fluorescence lifetimes, with averages of 4.76 ± 0.05 ns and 1.3 ± 0.2 ns. Figure 9(b) compares the corrected and non-corrected concentration estimates. The corrected estimates are approximately 1.4 times higher than the uncorrected concentration estimates. No differences in shape between the fluorescence spectra measured on the skin/muscle (by the F/R probe) and the liver and kidney were observed.

4 Discussion

The quantification of fluorophore concentration in tissue has typically been accomplished by comparing the measured fluorescence to a calibration curve developed from chemical extractions of biopsies from similar tissue sites.^{2,4,9} Rather than using tissue-specific calibration curves, we have examined the use of a single calibration curve from tissue-simulating phantoms to perform quantitative fluorescence measurements *in vivo*. We have also considered the possibility that the fluorescence quantum yield of our model fluorophore may be different *in vivo* than in the tissue-simulating phantoms. To account for a change in the fluorescence quantum yield we compared the time-resolved fluorescence decay measured in phantoms and in the tissue. In contrast to Vishwanath et al.,¹⁴ who found the fluorescence lifetime measured with a bundle of 100- μ m fibers did not depend on the optical properties of tissue phantoms, we observed a small dependence of the apparent fluorescence lifetime on μ'_s and μ_a when fluorescence was excited and detected using a single 200- μ m optical fiber in the

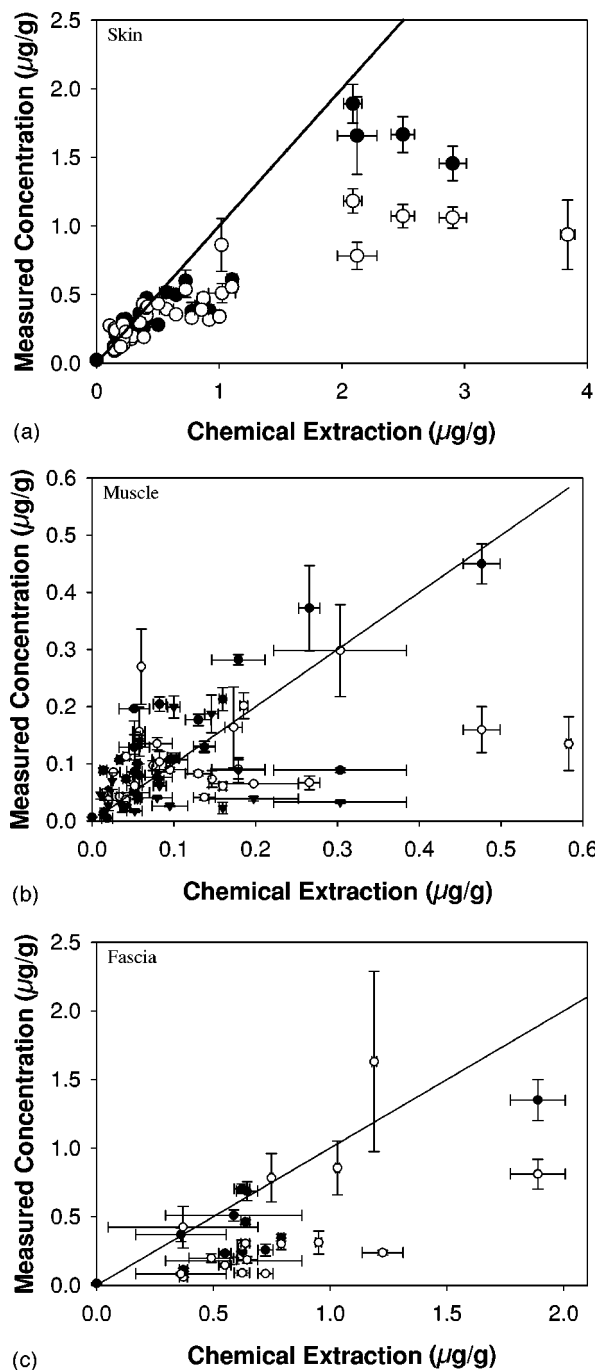
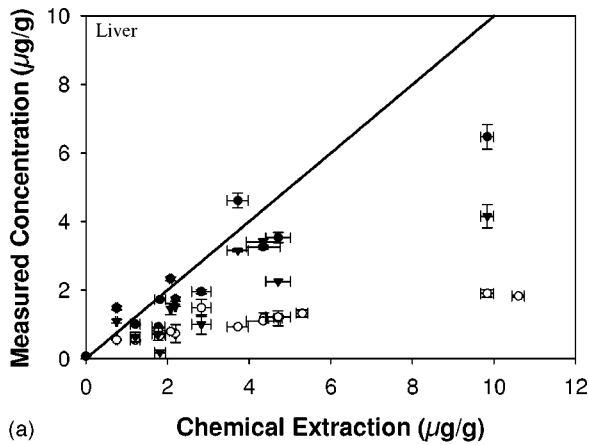
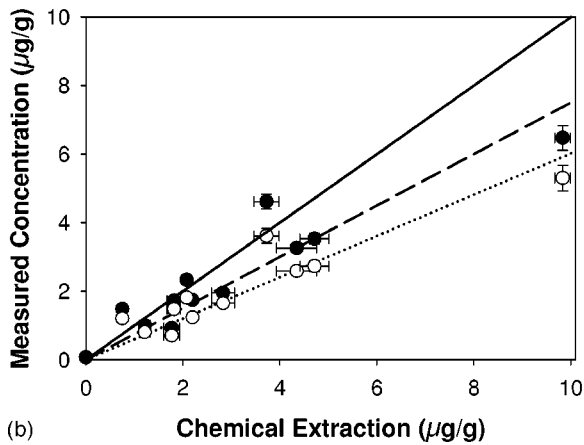


Fig. 7 ALPcS₄ concentration measured in (a) skin, (b) muscle, and (c) fascia. Closed circles represent surface measurements made with the single optical fiber, and open circles using the F/R probe. Inverted triangles represent interstitial measurements made using the single fiber, and the solid lines are the lines of equality. Vertical error bars are the standard error in the mean for at least three measurements repeated at the same location after removal and replacement of the probes. The horizontal error bars are the same as the vertical error bars in Fig. 5.

same geometry as Vishwanath (Fig. 3). Interstitial measurements of the lifetime were more dependent on the optical properties of the medium, likely due to an increase in the mean length of the path the fluorescence travels before detec-



(a)

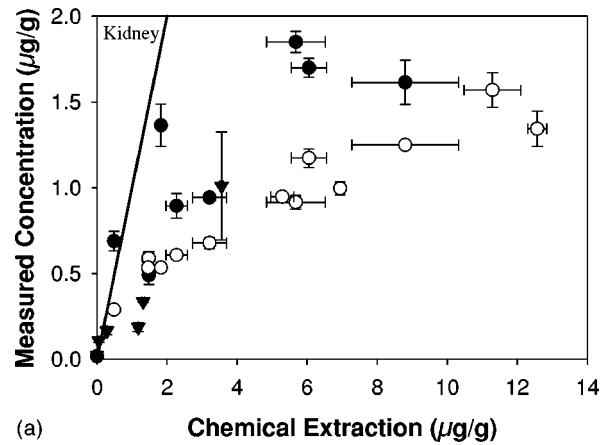


(b)

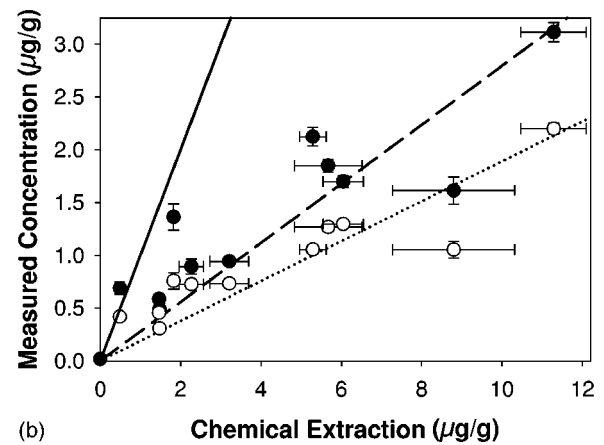
Fig. 8 ALPcS₄ concentration measured in liver. (a) Estimates for surface measurements with the single fiber (closed circles), the F/R probe (open circles), and interstitial measurements (inverted triangles). The effect of accounting for differences in the fluorescence lifetime is demonstrated in (b). Closed circles are the surface data for a single fiber, shown in (a); open circles show the concentration estimates that would be obtained by a steady-state measurement. Linear regressions are shown for the corrected (long dashes) and uncorrected (dotted) data. The ratio of the corrected and uncorrected slopes is 1.27. The solid line in each panel is the line of equality. The horizontal error bars are the same as the vertical error bars in Fig. 5.

tion. For highly scattering tissues ($\mu'_s > 2 \text{ mm}^{-1}$) the apparent increase in the fluorescence lifetime might obscure small differences between the tissue measurement and the calibration phantom.

The goal of this study was to ascertain if simple measurements of fluorescence could determine fluorophore concentrations *in vivo* using an independent calibration in a tissuelike medium. The literature regarding the retention of ALPcS₄ is somewhat inconsistent. There is a wide range of specific uptake in a variety of rodent models for each tissue site we measured. However, the specific uptake measured in these rabbits was comparable to earlier studies by our group.^{7,12} We found reasonable agreement between the measurements made with the F/R probe and the single optical fiber in the lighter colored tissues, although both tended to underestimate the tissue concentration at higher concentrations. The underestimation was greatest in the liver and the kidney, but the estimates



(a)



(b)

Fig. 9 ALPcS₄ concentration measured in kidney. (a) Estimates for cortex surface measurements with the single fiber (closed circles), the F/R probe (open circles), and interstitial medulla measurements (inverted triangles). Only five medulla samples were large enough for chemical extraction. The effect of accounting for differences in the fluorescence lifetime for cortex measurements is shown in (b). Closed circles are the surface data for a single fiber, shown in (a); open circles show the concentration estimates that would be obtained by a steady-state measurement. Linear regressions are shown for the corrected (long dashes) and uncorrected (dotted) data. The ratio of the corrected and uncorrected slopes is 1.4. The solid line in each panel is the line of equality. The horizontal error bars are the same as the vertical error bars in Fig. 5.

were improved for the single fiber probe by approximately 30% when a more appropriate instrument calibration was used ($\mu'_s \sim 1 \text{ mm}^{-1}$, $\mu_a \sim 0.2\text{--}0.5 \text{ mm}^{-1}$). Recalibration of the F/R instrument resulted in a modest improvement of about 5%. Any improvement must be weighed against the inconvenience of a separate calibration for highly pigmented tissues. The underestimation was not likely due to absorption of the fluorescence by the fluorophore itself, because the calibrations were almost linear out to concentrations of 5 $\mu\text{g/mL}$ in the tissue-simulating phantoms. Tissue autofluorescence was observed only in the liver but was not significant as demonstrated by the measurements on the control rabbit shown in Figs. 7, 8, and 9.

The probes were held in place by hand for all measurements, with care taken to hold them steady and normal to the surface. However it was sometimes difficult to maintain good

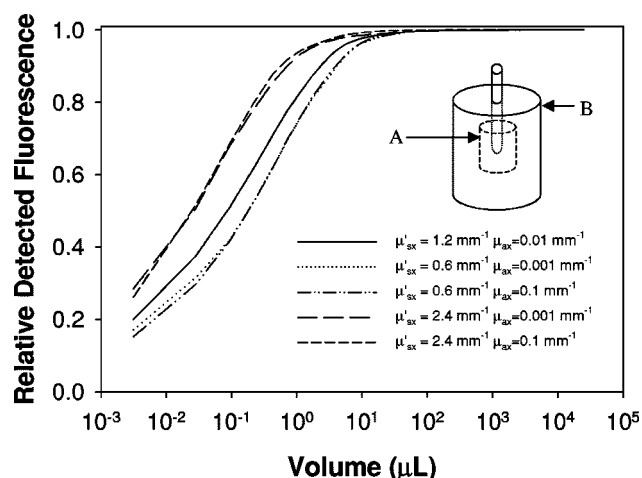


Fig. 10 Monte Carlo simulations of fluorescence excitation and detection by a 200- μm interstitial fiber. The volume on the abscissa is a cylinder centered on the tip of the fiber (with the fiber volume subtracted). The ordinate is the signal detected from this volume (A) divided by the signal from a 25-mL volume (B).

contact with the measurement surface. A gradual decrease in the count rate measured by the time-resolved instrument was often observed during a measurement. This was partially countered by switching to shorter integration times. We do not believe that this effect was the result of photobleaching, because repeated fluorescence measurements using the F/R probe (on any given site) did not exhibit a decrease in the fluorescence signal. Small amounts of blood seeped from the measurement sites on liver and kidney (both surface and interstitial measurements) as the single fiber probe was removed. We drew blood from three of the rabbits shortly before sacrifice. No fluorescence (in a standard 90-deg excitation/detection geometry) was observed from those samples. Thus any blood pooling near the source or detectors of either probe would tend to reduce the measured concentration. Previous work¹² showed good correlation between the concentration measured using a different F/R probe and chemical extraction, albeit for a single rabbit. In that case, anesthesia was maintained by a Ketalean®/Atravet® mixture. We measured four rabbits with injected doses of AIPcS₄ ranging from 0.5 to 4 mg/kg, and determined that the systematic underestimation was not associated with the mode of anesthetic delivery (and hence these data are not shown separately).

One drawback of measurement techniques that probe large volumes of tissue is that they are insensitive to smaller scale inhomogeneities in the fluorophore distribution. For example, using the single fiber probe we detected two different regions of uptake in the kidney (measured at the surface of the cortex and interstitially, in the medulla). To estimate how localized the measurement was, we performed Monte Carlo simulations of fluorescence excitation and detection by a single interstitial optical fiber (200- μm diameter) with 635-nm excitation and 680-nm emission wavelengths for 1 $\mu\text{g}/\text{mL}$ AIPcS₄ in turbid media with a wide range of optical properties. Figure 10 shows the relative fluorescence signal collected from a cylindrical volume centered on the tip of the fiber (the volume of the

fiber has been subtracted) for a wide range of optical properties as a function of the volume of that cylinder. The smallest volume represents a 100- μm diameter \times 100- μm -high cylindrical volume element centered on the tip of the fiber. It can be seen that in all types of tissue, the majority of the fluorescence signal arises from a volume less than 1 μL , and 95% of the signal from 4 μL or less. If the response is integrated over the radial direction it can be shown that 95% of the signal arises from a depth of 0.50 mm or less. This small sensitive volume probably contributes to the scatter observed in Figs. 7–9. It might also contribute to the systematic underestimation of concentration if the distribution in the organ of interest is not homogeneous. For example, the skin is 2 to 3 mm thick, so our measurement samples the outer 10 to 20% where the concentration could be different than that measured for a full thickness skin sample by chemical extraction.

One of the questions we addressed was whether a measurement of the fluorescence lifetime is useful for correcting for possible changes in the fluorescence quantum yield *in vivo* compared to the calibration standard. The results obtained during this study, while not necessarily applicable to other fluorophores and other animal models, raised interesting points. The fluorescence lifetime of AIPcS₄ measured in skin, muscle, and fascia was not significantly different from the lifetime measured in aqueous tissue-simulating phantoms. This suggests that quantification of AIPcS₄ in these sites could be performed using a simple steady-state measurement of the fluorescence. The multi-exponential decays observed in liver and kidney make these organs possible candidates for time-resolved or frequency domain measurements. In our rabbit model a 25% improvement of the concentration estimate in the liver and a 45% improvement in the kidney cortex was realized when the multi-exponential decay of the fluorescence was accounted for. However, it is important to note that a similar study should be repeated for other model systems and other fluorophores, such as Photofrin® or protoporphyrin IX (PpIX), if quantitative measurements are based on external standards.

In this study we demonstrated that the fluorescence measured *in vivo* using either a single optical fiber or the fluorescence/reflectance ratio method yielded good estimates of the fluorophore concentration for skin, muscle, and fascia at low concentrations. Results were not as reliable at high doses, especially for liver and kidney. For these organs it may be necessary to perform some kind of *in vivo* calibration, as in Ref. 9. The question remains as to why both of these instruments tended to underestimate the fluorophore concentration compared to chemical extractions. It is not clear whether the chemical extractions or the *in vivo* measurements were erroneous. One approach to answer this question would be to use radiolabeled AIPcS₄. The concentration estimated by the fluorescence-based techniques and the chemical extractions could be compared to the concentration determined by counting the radioactive decays from the excised tissue. This additional measure of concentration might suggest a mechanism for the systematic underestimation.

Acknowledgments

This research was supported by the National Institutes of Health, PO1-CA43892.

References

1. R. B. Dorshow, J. E. Bugaj, B. D. Burleigh, J. R. Duncan, M. A. Johnson, and W. B. Jones, "Noninvasive fluorescence detection of hepatic and renal function," *J. Biomed. Opt.* **3**, 340–345 (1998).
2. J. K. Frisoli, K. T. Schomacker, E. G. Tudor, T. J. Flotte, T. Hasan, and T. F. Deutsch, "Pharmacokinetics of a fluorescent drug using laser-induced fluorescence," *Cancer Res.* **53**, 5954–5961 (1993).
3. M. Gurfinkel, A. B. Thompson, W. Ralston, T. L. Troy, A. L. Moore, T. A. Moore, J. D. Gust, D. Tatman, J. S. Reynolds, B. Muggenburg, K. Nikula, R. Pandey, R. H. Mayer, D. J. Hawrysz, and E. M. Sevick-Muraca, "Pharmacokinetics of ICG and HPPH-car for the detection of normal and tumor tissue using fluorescence, near-infrared reflectance imaging: a case study," *Photochem. Photobiol.* **72**, 94–102 (2000).
4. M. Panjehpour, R. E. Sneed, D. L. Frazier, M. A. Barnhill, S. F. O'Brien, W. Harb, and B. F. Overholt, "Quantification of phthalocyanine concentration in rat tissue using laser-induced fluorescence spectroscopy," *Lasers Surg. Med.* **13**, 23–30 (1993).
5. W. R. Potter and T. S. Mang, "Photofrin II levels by in vivo fluorescence photometry," *Porphyrin Localization and Treatment of Tumors* **101**, 177–186 (1984).
6. S. L. Jacques, R. Joseph, and G. Gofstein, "How photobleaching affects dosimetry and fluorescence monitoring of PDT in turbid media," in *Optical Methods for Tumor Treatment and Detection*, T. J. Dougherty, Ed., *Proc. SPIE* **1881**, 168–179 (1993).
7. R. A. Weersink, J. E. Hayward, K. R. Diamond, and M. S. Patterson, "Accuracy of noninvasive in vivo measurements of photosensitizer uptake based on a diffusion model of reflectance spectroscopy," *Photochem. Photobiol.* **66**, 326–335 (1997).
8. J. R. Mourant, T. M. Johnson, G. Los, and I. J. Bigio, "Non-invasive measurement of chemotherapy drug concentrations in tissue: preliminary demonstrations of in vivo measurements," *Phys. Med. Biol.* **44**, 1397–1417 (1999).
9. C. C. Lee, B. W. Pogue, R. R. Strawbridge, K. L. Moodie, L. R. Bartholomew, G. C. Burke, and P. J. Hoopes, "Comparison of photosensitizer (AlPcS₂) quantification techniques: in situ fluorescence microsampling versus tissue chemical extraction," *Photochem. Photobiol.* **74**, 453–460 (2001).
10. B. W. Pogue and G. Burke, "Fiber-optic bundle design for quantitative fluorescence measurement from tissue," *Appl. Opt.* **37**, 7429–7436 (1998).
11. L. Lilge, C. O'Carroll, and B. C. Wilson, "A solubilization technique for photosensitizer quantification in ex vivo tissue samples," *J. Photochem. Photobiol., B* **39**, 229–235 (1997).
12. R. Weersink, M. S. Patterson, K. Diamond, S. Silver, and N. Padgett, "Noninvasive measurement of fluorophore concentration in turbid media using a simple fluorescence/reflectance ratio technique," *Appl. Opt.* **40**, 6389–6395 (2001).
13. K. R. Diamond, M. S. Patterson, and T. J. Farrell, "Quantification of fluorophore concentration in tissue-simulating media by fluorescence measurements with a single optical fiber," *Appl. Opt.* **42**, 2436–2442 (2003).
14. K. Vishwanath, B. Pogue, and M.-A. Mycek, "Quantitative fluorescence lifetime spectroscopy in turbid media: comparison of theoretical, experimental and computational methods," *Phys. Med. Biol.* **47**, 3387–3405 (2002).
15. D. E. Hyde, T. J. Farrell, M. S. Patterson, and B. C. Wilson, "A diffusion theory model of spatially resolved fluorescence from depth-dependent fluorophore concentrations," *Phys. Med. Biol.* **46**, 369–383 (2001).
16. J. R. Lakowicz, *Principles of Fluorescence Spectroscopy*, 2nd ed., Kluwer Academic/Plenum, New York (1999).
17. W. S. Chan, J. F. Marshall, G. Y. F. Lam, and I. R. Hart, "Tissue uptake distribution and potency of the photoactivatable dye chloroaluminum sulfonated phthalocyanine in mice bearing transplantable tumors," *Cancer Res.* **48**, 3040–3044 (1988).
18. C. J. Tralau, A. J. MacRobert, P. D. Coleridge-Smith, D. Akdemir, and T. J. Wieman, "Photodynamic therapy with phthalocyanine sensitisation: quantitative studies in transplantable rat fibrosarcoma," *Br. J. Cancer* **55**, 389–395 (1987).
19. S. G. Bown, C. J. Tralau, P. D. Coleridge-Smith, D. Akdemir, and T. J. Wieman, "Photodynamic therapy with porphyrin and phthalocyanine sensitisation: quantitative studies in normal rat fibrosarcoma," *Br. J. Cancer* **54**, 43–52 (1986).
20. W. S. Chan, J. F. Marshall, R. Svendsen, J. Bedwell, and I. R. Hart, "Effect of sulfonation on the cell and tissue distribution of the photosensitizer aluminum phthalocyanine," *Cancer Res.* **50**, 4533–4538 (1990).